Moly, a prototype hand-held 3D digitizer with diffraction optics

Tom D. Ditto[a*] and Douglas A. Lyon[b**]

[a] DeWitt Brothers Tool Company, Inc., PO Box 4000, Ancramdale, NY 12503

[b] Computer Science and Engineering Department, University of Bridgeport, Bridgeport, CT 06601

ABSTRACT

A working hand-held 3-D digitizer, Moly, is demonstrated. It is distinguished by a magnification feature which is made possible by special diffraction optics that minimize the perspective effects typical of conventional triangulation. As a result, this innovative device illuminates its target with a collimated laser projector that produces a sheet of light of uniform height at all working distances. The diffraction optics afford improved depth-of-field compared to triangulation scanners of equivalent resolution. This prototype also employs dual magnetic wave detectors to facilitate freedom of movement for both the digitizer and the subject. The instrument was designed primarily to digitize human faces and figures for applications in art and medicine.

Keywords: diffraction, range finder, holography, grating, 3-D, third-dimension, profilometry, machine vision, metrology.

1. BACKGROUND

The authors trace their experimentation with 3D digitizers back to our Pantomation [1] computer interface *circa* 1982, a spatial tracking system that used video camera transducers and a modified light pen architecture to follow real time movement. In 1983 Pantomation was used in conjunction with a theatrical laser projector to scan 3D surfaces. This early experimentation followed the strategy of triangulation and suffered from the limitations of perspective foreshortening, occlusion liability, and fixed field-of-view that are endemic to the triangulation method.

The weaknesses of triangulation led to the discovery of a new method of range finding based on diffraction that offered some potential improvements on these limitations.[2] A 1987 prototype demonstrated a synchronized scanning feature that can overcome the fixed field-of-view problem.[3] By this we mean that the camera and the projected laser beam were functionally coaxial wherever scanned. The prototype employed a type of surface relief plane grating that is commercially available as an inexpensive embossed plastic material. The diffraction method enjoyed redundant target views that reduced occlusion liability when compared to other published methods of synchronous scanning. However, perspective foreshortening remained a problem.

To overcome the perspective foreshortening and to further reduce occlusion liability, the authors have invented a diffraction optical element based on chirp gratings. Unlike the plane gratings used in our prior demonstrations, the chirp grating has a variable pitch. The change in pitch results in a magnification feature that can be tailored to target distance.

2. THEORY OF OPERATION

The diffraction method works on the principle that higher-order diffraction spectra are displaced relative to a central zero-order as a function of target distance. For this method to work, targets must radiate energy as periodic waves, although neither monochromatic nor coherent waves are requisite. Targets can be self-illuminated, or they can be designated by an interrogating beam, typically a laser to take advantage of its superior depth of focus. The energy is viewed through a diffraction grating. In the light regime, the transducer can be a video camera. In order to form higher-order images, a lens is placed between the grating and the transducer. The lens forms a perspective center through which rays can be traced from the transducer surface to the grating and thence from the grating to the target.

---

* Correspondence: e-mail: ditto@taconic.net; web http://www.dewittbros.com
** Correspondence: e-mail: lyon@DocJava.com;web: http://www.DocJava.com; phone (203)576-4760; 576-4766 FAX

Specification of a diffraction range finder that will produce a desired higher-order image displacement for a given target distance can be made using equations that are derived from the well-known Grating Equation

$$\sin(r) + \sin(i) = n\frac{\lambda}{p} \tag{1}$$

where r is the angle at which diffraction images are reconstructed
         i is the angle of incidence of a wave front
         n is the diffraction order, an integer
         λ is the wavelength of incident energy
         p is the pitch of the grating

In the near-field where the wave front striking the grating is appreciably spherical, angles i and r vary as a function of the range of the source. This is the basis of range finding by diffraction. A measurement of the angle r at a receiver at distance d from the grating will yield the range D of a target according to the relationship:

$$D = d\,\tan(r)\frac{\sqrt{1 - \left(n\frac{\lambda}{p} - \sin(r)\right)^2}}{n\frac{\lambda}{p} - \sin(r)} \tag{2}$$

In the regime of visible radiation, the receiving angle r is acquired using a camera with a lens of focal length F along a focal plane where a displacement x along one axis can be measured. In this setting it can be said:

$$r = \arctan\left(\frac{x}{F}\right) \tag{3}$$

A range camera devised according to this principle using a plane grating is illustrated below in Figure 1. Since we have parameters in equations (2) and (3) that can be known, measurements of displacement x of a higher-order image formed at the image plane can be correlated to a range distance, D. However, for any equal displacement x distances D increase geometrically as a function of range. This effect is called perspective foreshortening, a parabolic shaped dependency of displacement of higher-order diffraction images as a function of target range which is also characteristic of triangulation range finders.
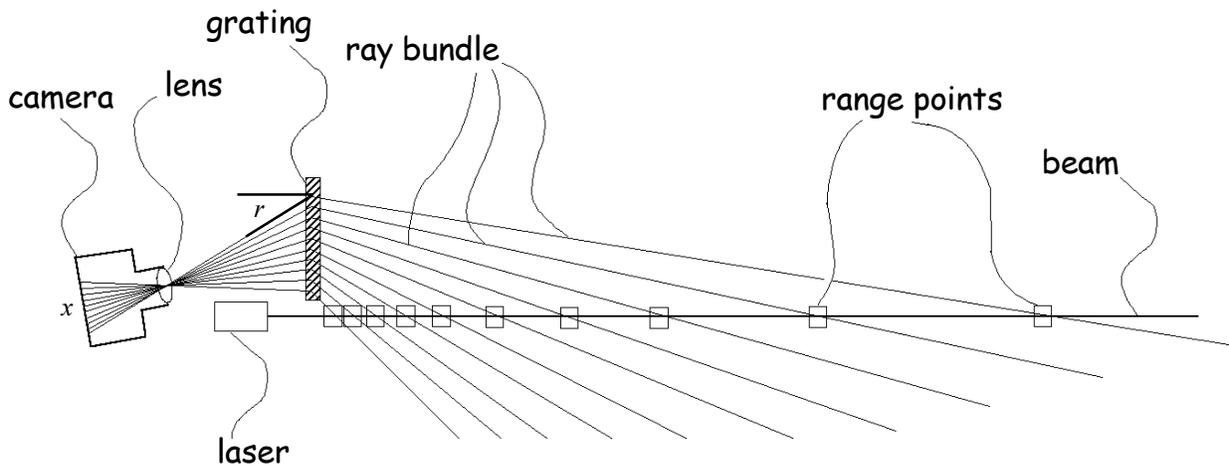
Figure 1 - A diffraction range finder using a plane grating. In the diagram, rays are placed in equal steps along a camera focal plane. Note that corresponding range points are not in equal steps but increase geometrically in spacing as a function of range.

It is possible to alter perspective foreshortening by changing the pitch of the grating along its length. We can express the angle of incidence of a ray upon the diffraction grating as

$$i = \arctan\left(\frac{xd}{FD}\right)$$
(4)

Substituting equations (3) and (5) we can solve for p in equation (1).

$$p = \frac{n\lambda FD}{2xd}\sqrt{1+\left(\frac{xd}{FD}\right)^2}$$
(5)

Using this equation, an arbitrary displacement x on the focal plane of a camera and an arbitrary distance D of a target a grating pitch will determine an appropriate grating pitch, p.
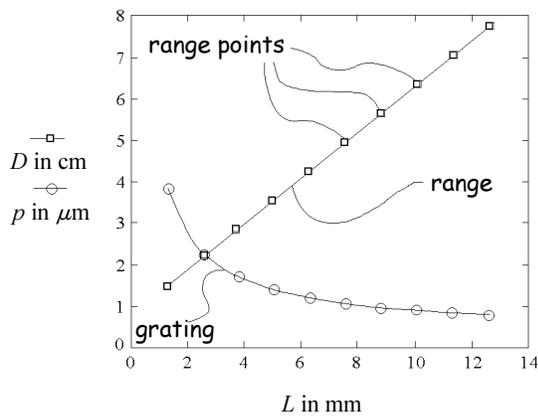
Figure 2 - Graphs of range D vs. position L along a grating compared with the corresponding pitch p of the grating at position L.

Using this dependency, we can model gratings that would show a linear displacement of diffraction images as a function of even steps of range distances. The resultant grating models are variable pitch gratings with a hyperbola shaped wave length chirp.

To graph this relationship, we calculate an abscissa in terms of position along the grating length L where $L = \frac{xd}{F}$ (6).

Figure 2 to the left shows a typical specific calculation which is applied to the camera model shown below in Figure 3. As range distance changes, the displacement along the focal plane of the camera changes in a linear relationship. In order for this to work, the pitch (i.e. wave length) of the grating must increase as the distance increases. The rate of change in the pitch is itself hyperbolic and not linear.
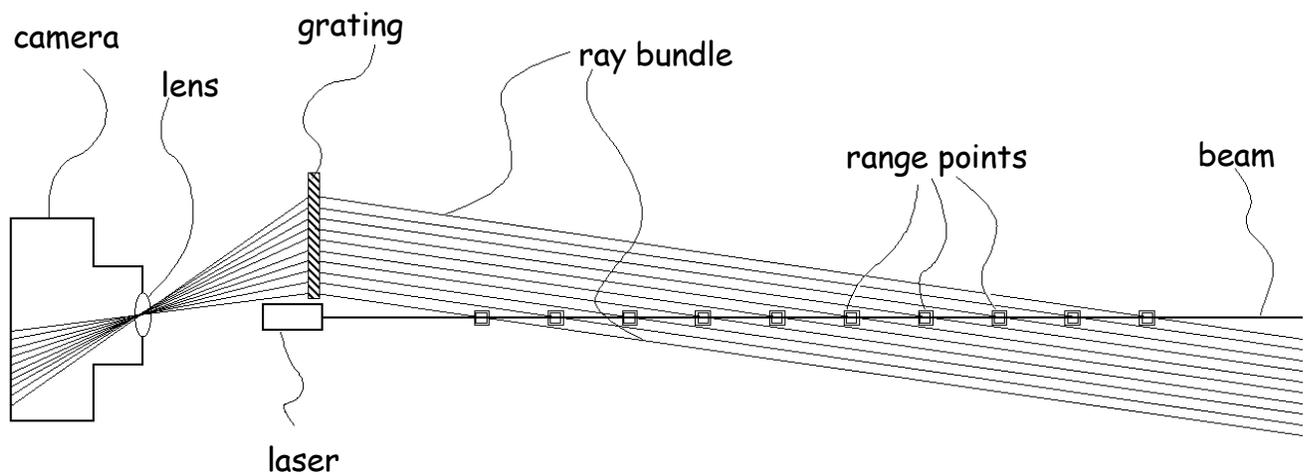
Figure 3 - A diffraction range finder using a chirp grating designed to linearize the relationship between range distance and displacement of the higher-order diffraction image along the focal plane of a camera. The box tick marks correspond to the graph in Figure 2 above.

3. MOTIVATION FOR MOLY

We had previously built a prototype synchronous 3D scanner using a plane grating, but the chirp grating did not afford us this synchronous scanning option which had utlitized a mirror mounted on a galvanometer. We now contemplated a hand-held unit that assumed interactive scanning by the user. Devices of this type must have a *localizer*, that is, a reference point on the scanner that is tracked relative to the coordinate space of the subject being scanned. From the available options for localization we chose magnetic wave detection, a technology that was compatible with our intended subjects of human faces and figures.

Magnetic wave detectors enjoy occlusion immunity which is superior to line-of-sight methods based on triangulation, but the magnetic field is subject to distortion by conductive metals. As a result, our machinist, Paul Friedlander, chose a plastic material, molybdenum di-sulfide impregnated nylon for the construction of our scanner from which he coined a name for our prototype, "Moly."

We know from the history of 19th century photography that special problems arose when subjects had to remain motionless during the long exposures required by early photographic recording materials. As a hand-held profilometer we foresaw a similar problem with Moly, since it would be acquiring merely a 200 mm line profile over each 33 ms and would therefore require many seconds to fully scan a face or other body feature. To allow the subject some freedom of movement, we developed a dual localizer system, one for the scanner and another that could be fixed on the subject. With this adaptation, the subject would generate a coordinate space relative to Moly. Indeed, even with Moly stationary, a subject could scan himself through his own movement. While we were working on our dual tracker, we learned of a similar system for a triangulation-based profilometer which is now marketed by Polhemus[4],the manufacturer of our localizer.

We used the metaphor of a "3D Paintbrush" to guide our design. The bristles of our paintbrush were virtual. They sensed a profile taken along a stripe of illumination projecting from the scanner. The metaphor introduces a design constraint not found in triangulation sensors where the projection system is typically conical in shape, that is, originating at a point and expanding at some projection angle. We learned from users of triangulation systems that the expanding field-of-view typical of their laser projectors was difficult to handle, because in the near field the acquisition stripe was smaller than a longer acquisition stripe in the far field. Our projection system was going to be more difficult to build but offered the user a functional improvement when compared to typical triangulation systems.
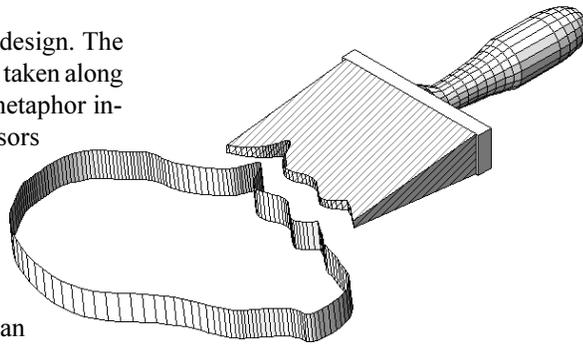
Figure 4 - The 3D Paintbrush Concept

Our design required an optimization of occlusion liability, the angle inscribed between a projected laser line and a corresponding sight line at the receiver. In a triangulation system the extreme case would be a 90 degree separation, in which case the camera sees a 1:1 profile, that is, a sideway's view. However, such a radical angle is impractical, calling for the camera to be embedded inside the target in most instances. In commercially available triangulation systems, the occlusion liability angles are rarely greater than 45 degrees. We settled on a 16 degree occlusion liability angle. This is an improvement over most commercial triangulation systems, where a 28 degree angle is a benchmark. Moreover, unlike triangulation systems, the occlusion liability angle in Moly would be constant, because the sight lines to the receiver would be parallel.

Of course, we could not proceed without a diffraction grating made to our specification, and here we faced the greatest challenge. Unlike plane gratings, chirp gratings are not commonplace in spectroscopy and cannot be bought off-the-shelf. Yet we knew that every hologram is itself a complex diffraction grating, so we turned to holographers to make our grating. Our ignorance of the process proved to be one of the most interesting turns in the project, because we took it on advisement from our first subcontractor that a hyperbolic chirp was *not* an option if the grating was made holographically. We learned later that, in fact, a hyperbolic chirp is the *only* option in a simple holographic grating, but in our confusion we developed design tools which were premised on the notion that the chirp rate would be linear. We also came to respect the problems of grating efficiency. Our first proposed design looked almost exactly like the paintbrush in Figure 4 above, but the diffraction angles were so shallow that the gratings proved extremely inefficient. As our expertise grew, we learned that the safest way to design an efficient grating was to have the diffraction occur near the Bragg angle, and this informed the design of Moly.

4. DESIGN TOOLS

We developed two routes to design our optical system, classical trigonometry and interactive computer software. We felt that having corroboration between the two types of model would give us better confidence when we committed to a grating specification.

The classical geometric optics of diffraction range finding have been alluded to in the theory **Section 2** above, but the devil is in the details. If the occlusion angle is to be lowered, it helps to rotate the grating relative to the principal ray of the camera. With the grating inclined, the number of grooves used increases, the resolution increases, and also the Bragg angle is more easily achieved. An entry for this rotation which we call ρ must be included in our calculations. For best results using holographic materials, ρ should about 45 degrees. Here it is 41 degrees. Furthermore, in the tabulations that follow below as Figure 5, we have assumed a ½ inch CCD with a 16mm focal length lens. The target is illuminated by a laser diode with a wavelength of 636 nm that is rotated relative to the grating plane by 22 degrees, an angle we call α. Our grating has a linear chirp from 450 nm to 550 nm over its length L of 12.7 cm, the long side of the 4 x 5 inch holographic plate to be used. A stand-off along the grating plane to the laser of 12 cm is also factored in as the variable s.

A computer program, MathCad 6 was used for these calculations, hence the peculiar subscript j (an iterator) and operator convention $:=$ which is MathCad's symbol for equality. DL1 is range distance in this calculation and is calculated as a function of changes in x, the position of the diffraction image formed at the camera focal plane.

$$DL1_j := \frac{\left[\dfrac{\sqrt{1 - \left(n1 \cdot \dfrac{\lambda}{p_j} - \sin\left(\rho 1 + \mathrm{atan}\left(\dfrac{x_j}{F}\right)\right)\right)^2}}{n1 \cdot \dfrac{\lambda}{p_j} - \sin\left(\rho 1 + \mathrm{atan}\left(\dfrac{x_j}{F}\right)\right)}\right] \cdot \left(d1 \cdot \tan\left(\rho 1 + \mathrm{atan}\left(\dfrac{x_j}{F}\right)\right) - s1\right)}{\cos(\alpha 1) - \left[\dfrac{\sqrt{1 - \left(n1 \cdot \dfrac{\lambda}{p_j} - \sin\left(\rho 1 + \mathrm{atan}\left(\dfrac{x_j}{F}\right)\right)\right)^2}}{n1 \cdot \dfrac{\lambda}{p_j} - \sin\left(\rho 1 + \mathrm{atan}\left(\dfrac{x_j}{F}\right)\right)}\right] \cdot \sin(\alpha 1)}$$

Left graph: vertical axis $\dfrac{DL1_j}{cm}$ ranging 0 to 40 (with 20 marked); horizontal axis $\dfrac{x_j}{mm}$ ranging -4 to 4.

Right graph: vertical axis $\dfrac{\beta}{deg}$ ranging 14 to 18 (with 16 marked); horizontal axis $\dfrac{x_j}{mm}$ ranging -4 to 4.
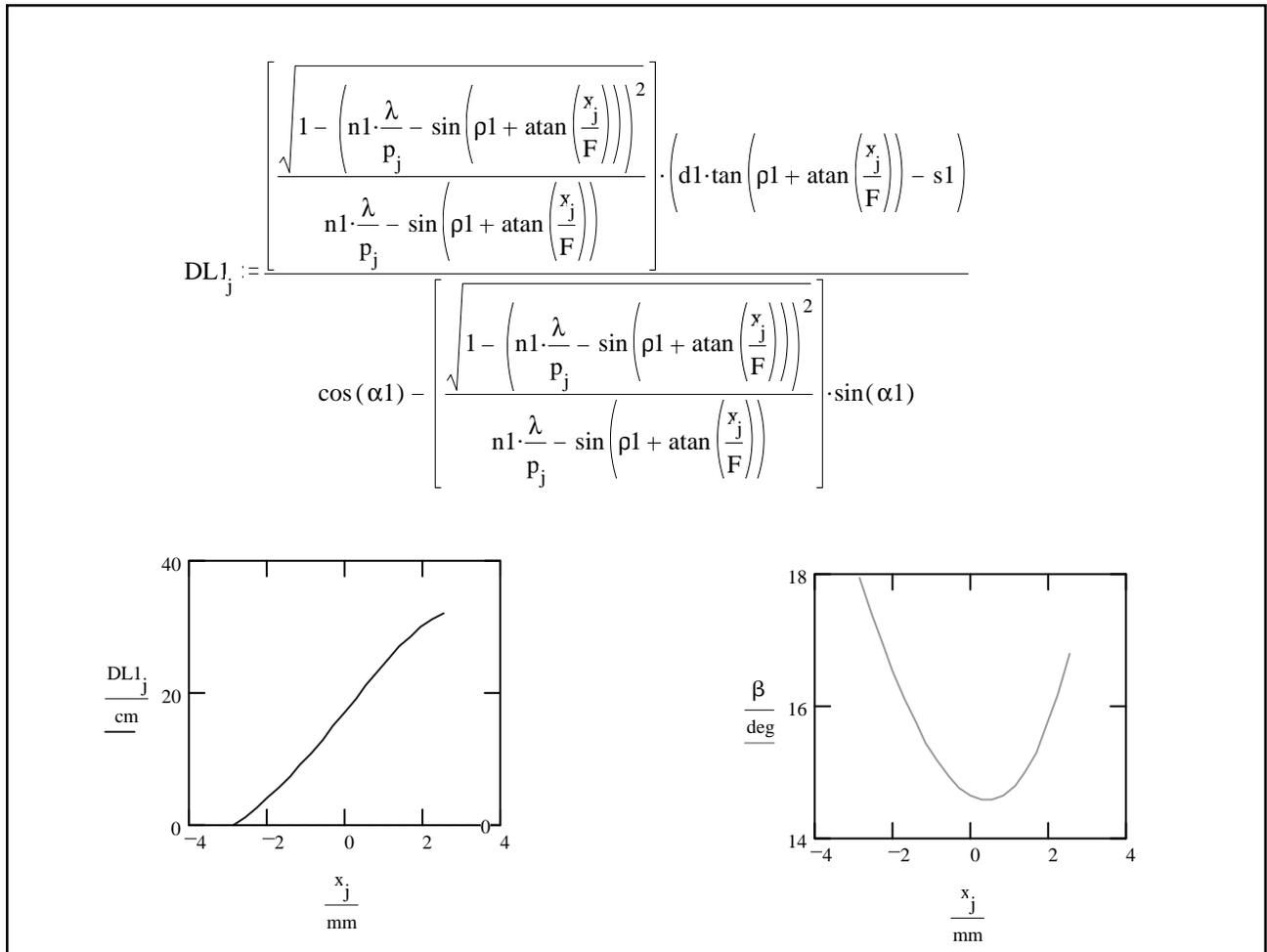
Figure 5 - Predictions of performance for an optimized grating with a linear chirp upon which Moly was based. The slight non linearity in DL1, the range, vs x, the diffraction image position, is due to the approximation that the grating has a linear rather than a hyperbolic chirp. The predicted occlusion liability angle, β, is also graphed.

DiffCAD is a program written in JAVA by Douglas Lyon and takes its name from the exercise of writing a diffraction computer-assisted design program. Later expanded to demonstrate JAVA coding for many signal processing algorithms, DiffCAD is distributed in a JAVA programming textbook [5] and as shareware on the DocJava.com web site. The user can specify the pitches of a grating at the *extrema*, and the program calculates the grating pitches across the surface as a linear chirp. A camera can be specified with one dimension of the sensor array and the lens focal length. The angle of view of the camera can be input or can be set automatically by the program as the user drags a camera icon with a mouse. The work area is has a user controllable grid for dimensioning, but many readings are returned in dialog boxes including graphs.

DiffCAD corroborated the predictions of the geometric optics equations developed in the MathCAD environment. In Figure 6 we see the original plan for Moly as rendered on the DiffCAD screen.
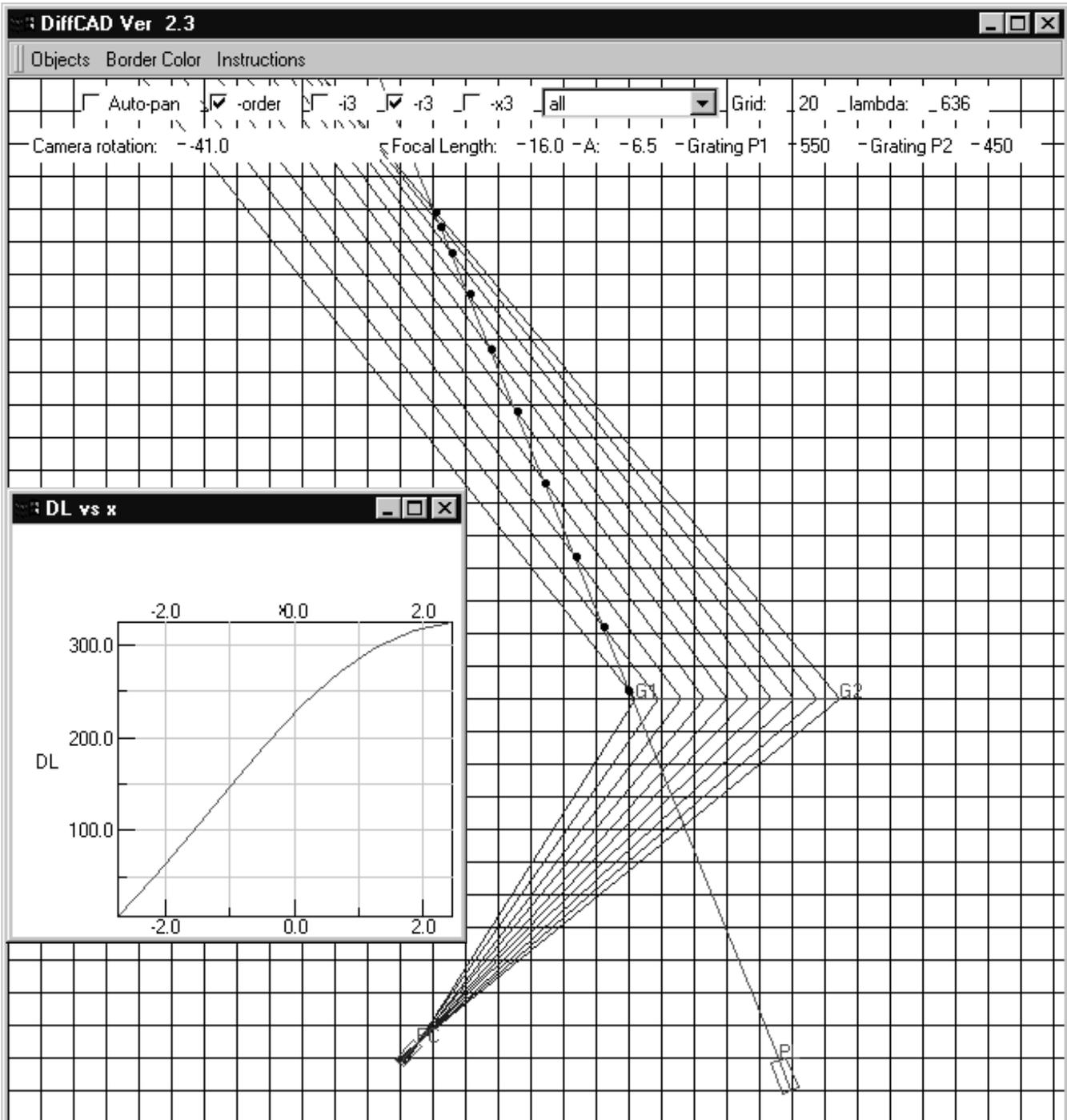
Figure 6 - The DiffCAD model of Moly. The laser, PL, intersects the sight lines from the grating at range points, and these are used to graph the range distances as recorded on a camera sensor. The grid is on 20 mm centers. Graph units are in mm.

5. THE ACTUAL PROTOTYPE

Our optical design tools did not account for the mechanical design of the instrument. Here we turned to a professional sculptor, Paul Friedlander [6], who is well versed in prototype assembly. This resulted in a pencil-on-paper plan that was realized in his machine shop.
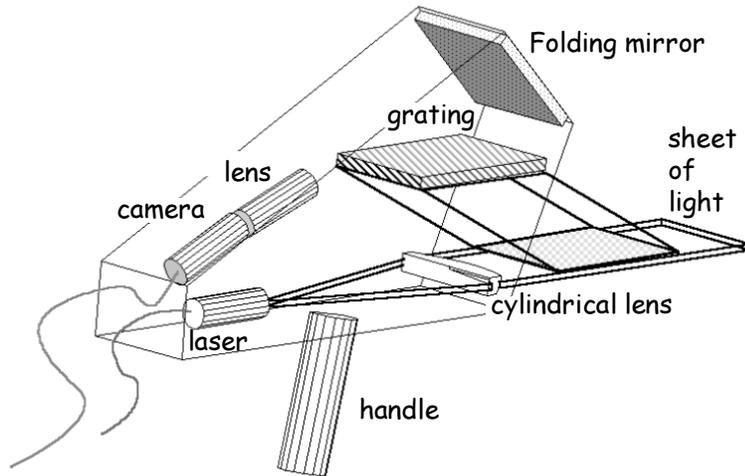
Figure 7 - Moly schematic showing the folding mirror that allows the camera to be next to laser line projector. The sight line from the grating intersects the laser sheet of light.

The design, illustrated to the left in Figure 7, incorporates a folding mirror which allowed the laser and camera to share a common location in the assembly. The camera and its lens were separately mounted on rails to allow for adjustments, especially the rotation of the lens relative to the camera sensor. This adjustment, the Scheimpflug angle, is critical to depth-of-focus in diffraction as well as triangulation range finders. We learned empirically that a five degree rotation was effective. To create a collimated laser beam, we used a laser with an integrated line projector and a cylindrical lens with a focal length matched to the 20 degree fan of the line projector. The resultant projection is a rectilinear sheet of light which matches the rectangular field of view from the grating.

The proof of the pudding is in the eating. Moly ended up being larger and heavier than we would have hoped. However, while not a paint brush, the chassis is similar to a vintage camcorder, a hand-held unit from our recent memory. At 3 kg, the unit is not steady in one hand but easily stablized when both hands are used. The size is traceable to the 170 mm stand-off between the laser and the cylindrical lens. This is matched by a nearly equal stand-off from the camera to the grating. The weight is due, in part, to the grade of plastic used for the walls. Even cut back with open sides, as illustrated to the right in Figure 8, it is a very dense material. The grating itself does not add significantly to the weight. Holograms are essentially flat and their only mass is their substrate. Here it is a 4x5 inch photographic plate. We chose a lipstick style CCD for its small size. Diode lasers are now ubiquitous and of stub pencil size. Miniaturization from Moly's dimensions appears to be realizable in future iterations.
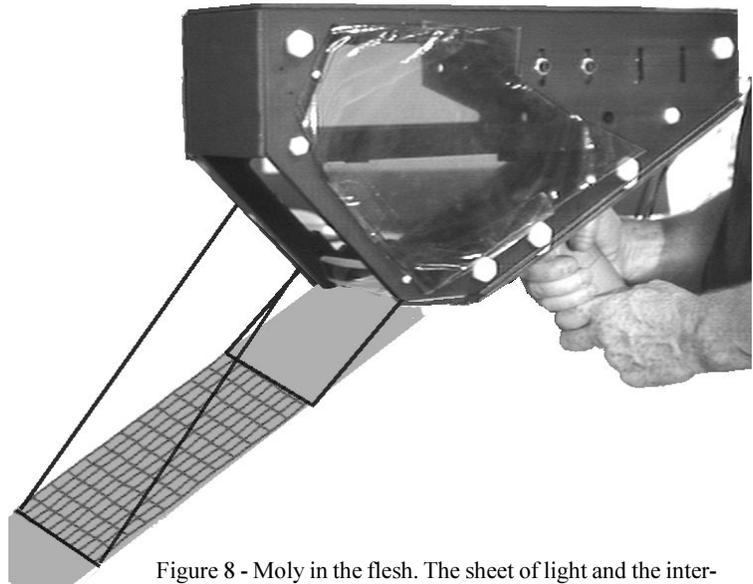
Figure 8 - Moly in the flesh. The sheet of light and the intersection with the sight line from the grating have been drawn in.

Not only was Moly a little larger than planned, its actual specifications differ from our original design, as well. As originally specified, range data would be available from point-of-contact with the grating, but we opted for a 10 cm stand-off from the body of the scanner to the nearest target to allow for some operator clearance. This shortened the total region of acquisition and raised the occlusion liability angle. As a further motivation, bench tests with the physical grating had shown that an occlusion liability angle of 15 degrees considerably degraded resolution. We selected the 28 degree angle occlusion liability angle that is widely adopted in triangulation scanners. This change in specification was also motivated by the realization that few targets have profiles over a 100 mm profile line of more than 200 mm, so a 300 mm deep scanning region, as originally specified, was probably not needed anyway. A 200 mm range depth has been born out as sufficient in our practice to date.

Our predictions did not include a model for grating efficiency other than to assure that the diffraction images would form near their Bragg angles. Indeed, holography is as much an art as a science, and of the three silver halide holograms made for Moly, one was far more efficient than the other two. However, all the gratings formed their diffraction images at +/- 5 degrees of the Bragg angle as indicated in Figure 9 to the right. We do not have efficiency figures, but Moly meets the test of performing within Class IIa laser illumination with a peak intensity of 0.5 mW along its projected stripe.

We also learned that the linear chirp model was incorrect, although it is a close approximation over the pitch spread we used. On the basis of our linear chirp model, we had expected a small amount of far field magnification, and we wished to use this as an argument for the diffraction range finding method. Triangulation systems suffer from loss of resolution caused by perspective foreshortening, and our perspective "farshortening" breaks with prior art in optical range finders. As it happens, we were able to introduce this effect in a subtle manner by moving Moly's camera back slightly from its originally specified location.

Figure 9 - Deviation from the Bragg angle $d\psi$ as a function of range distance.

The lens we use is unusual. Advertised as a "pin hole" lens [8], it actually is a conversion of a zoom microscope designed in such a manner that the ray bundle inverts in front of the first element. As a result, we can empirically determine the perspective center outside the lens, a blessing for prototyping. Moreover, it appears that the narrow pin hole serves to limit an astigmatism endemic to chirp gratings in our range finding configuration, because when we substituted a lens of equivalent f-stop and focal length, there was considerable blurring.

Our sensor is an American standard ½ inch CCD video camera rated at 570 horizontal lines of resolution. The "lipstick" package used puts the video processing in an outboard module connected by an umbilical. In Figure 10a below we show the video image captured in a 640 x 480 digitizer of a test bed made with a 50 mm wide target in 10 mm steps over a 180 mm range. For measurement we add a grid in Figure 10b.

Figure 10a - Calibration table scan. Near-field on left hand side. The target is placed in 10 mm steps from 100 to 300 mm from point-of-contact with Moly.

range axis ———⟶
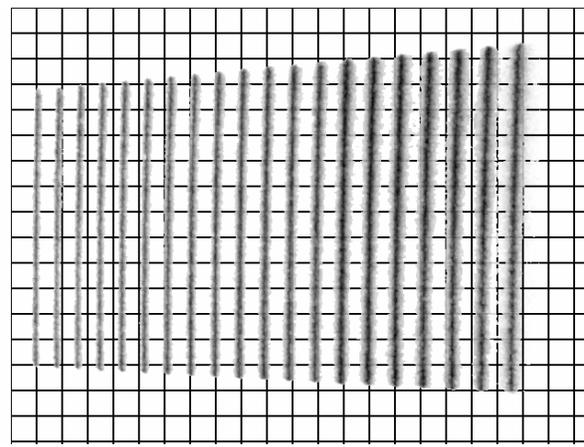
Figure 10b - Negative of Figure 10a with superimposed grid on 30 pixel centers..

Moly suffers from some sources of noise and geometric error. There are speckle artifacts from laser illumination. This is one drawback to employing a structured illumination source based on coherent readiation. Unique to our holographic grating is the magnification both in the horizontal (the dimension from which range information is extracted) and the vertical. Note how the stripeson the left fall slightly inside the 30 pixel grid lines while those on the right exceed the width of the grid lines. This pseudoscopia is deliberate, that is, the slight magnification with range distance was intended. However, the vertical magnification was unexpected. It is attributed to a keystone effect. The camera is viewing the grating at such an angle that the far field image is formed by a smaller section of the grating than the near field. Finally, there is a noticeable rotation in the target which is caused by a slight error in the angle of Moly's folding mirror relative to the grating plane.

The interface between Moly and the computer is a special peripheral card called SURFA by its manufacturer [7]. The card is not a typical framestore but rather functions by blocking all data at the input that is not above a user-set threshold and then storing only the filtered data stream in a FIFO pipeline for processing by an onboard DSP. The card samples data on alternate video fields and downloads the resultant data on a ISA type PC bus where it is handled by an Windows NT program called ModelMaker. A custom algorithm for intrapixel estimation produces range data in the DSP on the SURFA card itself. Calibration software in ModelMaker characterizes the range finder's performance. Moly achieved an RMS error of from 0.1 to 0.2 mm over a 100-300 mm range as detailed in the table on the right. The RMS error is based on multiple scans and shows the repeatability of the scanner system including the error introduced by the calibration system. These tests were conducted using a 60 mm wide target block which was moved along a lathe bed that was calibrated to 0.01 inch. Much of the RMS error may have been introduced by the lathe. We infer from the Range Error measurement that any one individual scan line showed a 10-30 micron optical resolution.

Camera Coordinates		Mean Width	Mean Z	Range Error	RMS Error
27	230	59.517	-0.288	0.009	0.19
32	232	60.007	20.25	0.008	0.312
37	233	60.13	40.925	0.025	0.182
42	234	60.124	60.997	0.007	0.086
47	235	60.06	81.262	0.012	0.09
51	236	60.347	101.585	0.014	0.106
56	237	60.186	121.911	0.006	0.092
60	238	60.32	142.178	0.07	0.244
65	239	59.762	162.631	0.032	0.211
69	239	59.851	182.578	0.049	0.221
72	239	59.869	203.087	0.019	0.18

Figure 11 - Calibration table produced by the ModelMaker program. All measurements are in mm.

In any event, the accuracy of Moly's optics appear to be well within the boundary set by its magnetic wave localizer which is rated at 1 mm accuracy over a meter hemisphere. Localizer error, therefore, is the primary dimensional distortion in Moly's real world scans. We tested Moly with a mannequin head, "Biff." We look forward to perfecting the art.
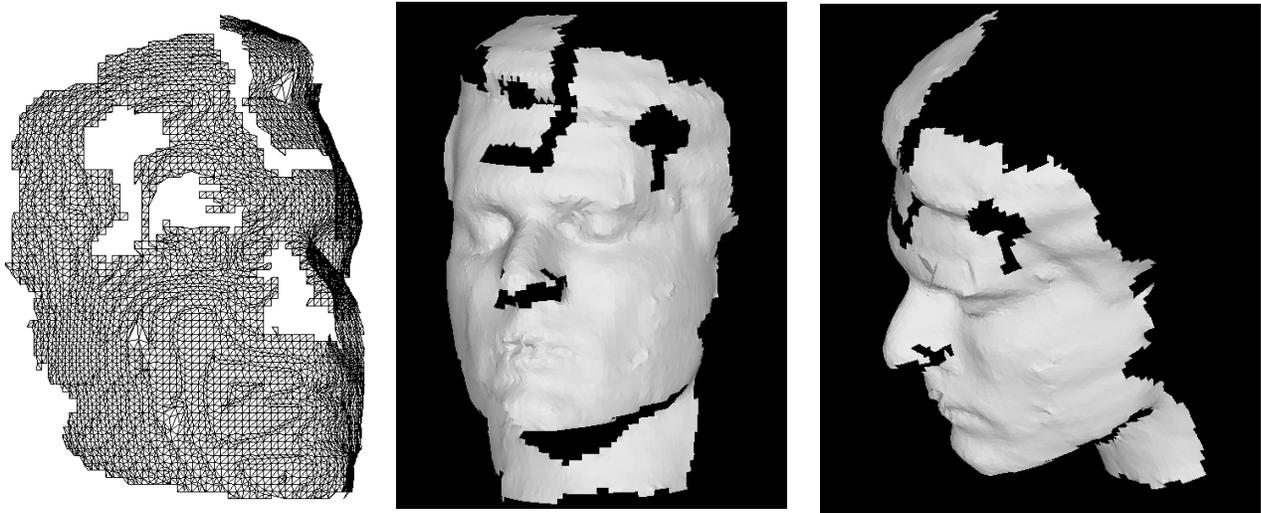
Figure 12 - The first scan of a head made with Moly. Occlusion artifacts and drop outs notwithstanding, we recognized the face.

6. LESSONS LEARNED AND SUGGESTIONS FOR FUTURE WORK

Our principal interest being diffraction range finding, the most pressing lesson learned from building Moly was to correct the far field vertical magnification effect created by Moly's camera angle. Note that in Figure 7, a schematic of Moly, the rays from the camera to the grating are not traced. Indeed, we had failed to take this ray path into account. Had we done so, it would have revealed the keystone effect caused by looking at the grating from off to the side. The question we now faced was whether moving away from the Bragg angle would result in an unacceptable loss of grating efficiency. We commissioned test gratings from holographic artist, Rudie Berkhout [9], with the specification that principal ray from the camera lens be perpendicular to the grating plane, Figure 13a. To produce this grating, he intersected a plane wave from off axis with a spherical wave perpendicular to the grating plane. The holograms he produced proved as efficient as Moly's, particularly those made where the plane wave was inclined at 60 degrees off the normal to the grating plane. However, the gratings were only efficient when rotated 10 degrees off the exposure plane, Figure 13b.
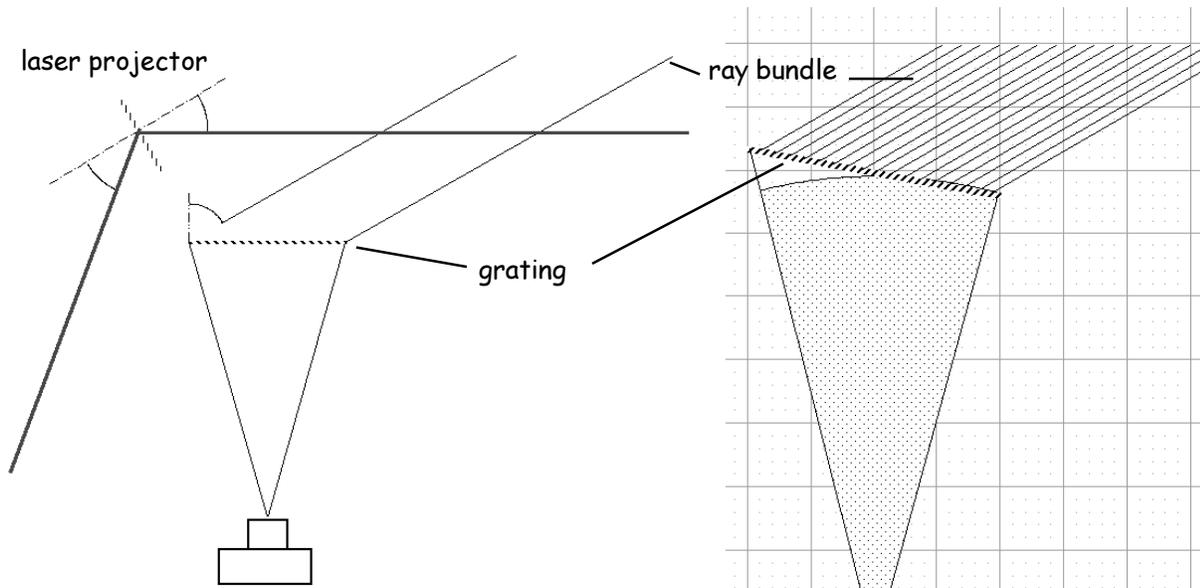
Figure 13a - Specification for grating with no keystone distortion in the camera pickup
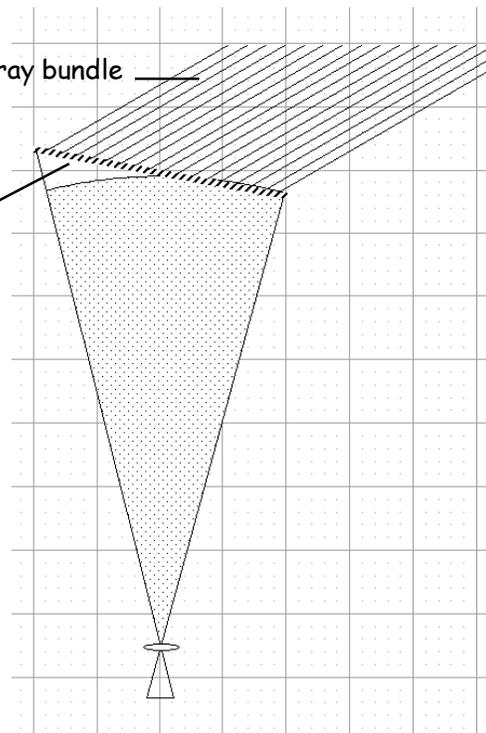
Figure 13b - Actual performance of grating

Another area of investigation is the potential for a 1:1 optical reproduction of range depth. In Figure 13a above, note how the laser projection beam runs parallel to the grating plane. Although it is interesecting the ray bundle at a nominal 30 degrees occlusion liability angle, the camera will record depth information as if were looking at the target from 90 degrees.

We used a Berkhout grating in a trial. Our target was a step block. Figure 14 show the block as photographed from the side with the acquired diffraction range image superimposed, and they are a good match. The occlusion lliability angle is actually 40 degrees, because the grating was rotated an additonal 10 degrees as per Figure 13b. By way of contrast consider the triangulation range image in Figure 15, made with the same test block at the same stand-off with the test block rotated to a 45 degree occlusion liability angle. The triangulation image shows perspective foreshortening even as it suffers a greater occlusion liability.

If an increase in occlusion liability can be tolerated, the method can be used to magnify beyond 1:1 by intersecting the structured light beam in an orientation perpendicular to the ray bundle. With diffraction angles approaching evanescence (90 degrees), such an approach promises to provide a means for 3D microscopy. Such improvements may rest with the exploitation of grating materials other than silver-halide depleted holographic plates. In this regard, we intend to investigate surface relief gratings, in part because they hold the promise of mass repllication.

Figure 14 - Test block with a grating image made at a 40 degree occlusion liability superimposed inside the rectangle
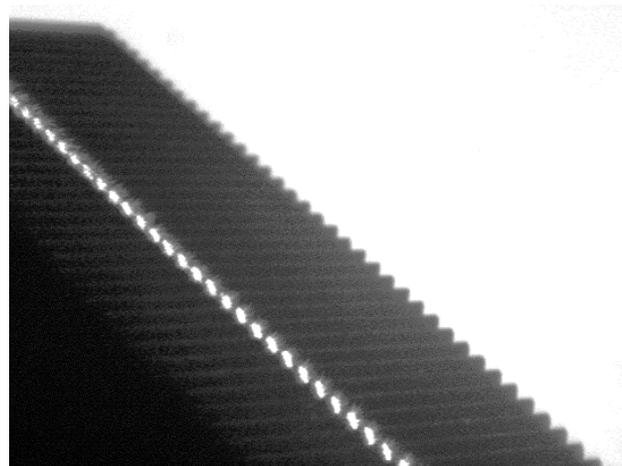
Figure 15 - Test block with triangulation image made at 45 degrees

As a computer vision device, the diffraction range finder must be integrated with software. Our research includes a software development component. In particular, the JAVA software that was pioneered in DiffCAD has been expanded to include scanner control, image processing and 3D rendering applets.

The instrument in Figure 16 to the right, which was used to make the image in Figure 14, is now resident at the University of Bridgeport where experimentation continues with a variety of localizer mechanisms other Moly's magnetic wave detectors. A rotary table and an x-y table have been used under embedded JAVA control to produce a series of scans which have been rendered in wireframe and texture mapped imagery as exampled by the illustration below, Figures 17.

Figure 16 - Grating, camera, and laser projector assembly

Figure 17 - Chess piece scanned on rotary table rendered with marble texture in JAVA

There are other avenues of research and development now being pursued. A license has been issued for the use of the diffraction range finder technology to Dimension Data [10] of Novi, Michigan aimed at the production of metrological instruments for use in the health and manufacturing sectors. The authors also have long term interests in the graphic arts, and variations of Moly could find their way into the production of computer animation. Most of the contributors to our project also have professional credentials in the visual arts and music. This could not have been a coincidence.

ACKNOWLEDGEMENTS

REFERENCES

[1] "Pantomation Demonstration," *SIGGRAPH Video and Film Review*, Vol. 2, Section 9, 1982
   also, DeWitt and Edelstein, "Pantomation - A System for Position Tracking, "*Proceedings of the Second Symposium on Small Computers in the Arts*, IEEE Computer Society, No. 455, pp. 61-70 and Tom DeWitt, "Pantomation Interface for the Apple II," *Proceedings of the Third Symposium on Small Computers in the Arts*, IEEE Computer Society, No. 499, pp. 25-29

[2] Thomas D. DeWitt and Douglas A. Lyon, "A Range Finding Method Using Diffraction Gratings," *Applied Optics*, May 10, 1995, Vol. 34 No. 14, pp. 2510-2521

[3] Unpublished videotape available from Tom Ditto, ditto@taconic.net
   Prior art in synchronous scanning methods is well exampled by Marc Rioux, "Laser range finder based on synchronized scanners," *Applied Optics*, Vol. 23, No. 21, pp. 3837-3844, 1984

[4] http://www.polhemus.com/hls1.htm
   also   http://www.aranz.co.nz/

[5] Douglas A Lyon and Hayagriva V. Rao, *JAVA Digital Signal Processing*, M&T Books, 1998, ISBN 1-55851-568-2

[6] http://www.praskovi.clara.net

[7] http://www.3dscanners.com

[8] http://www.mars-cam.com/frame/pinhole/v-zpl-xx.html

[9] http://www.rudieberkout.home.mindspring.com

[10] http://www.steinbichler.com